

Some Features of Dye-sensitized Solar Cell Combining with Single-walled Carbon Nanotubes[†]

Sanghun Lee, Hyunjune Park, Taehee Park, Jongtaek Lee, and Whikun Yi*

Department of Chemistry and Research Institute for Natural Science, Hanyang University, Seoul 133-070, Korea

*E-mail: wkyi@hanyang.ac.kr

Received November 13, 2013, Accepted January 3, 2014

A dye-sensitized solar cell (DSSC) was fabricated with a nanocrystalline TiO₂ film electrode on FTO glass, N719 dye, electrolytes (or CsSnI₃), and counter Pt electrode by incorporating it with single-walled carbon nanotubes (SWNTs). SWNTs were combined with TiO₂ film, CsSnI₃, Pt electrode, separately, and the SWNT-containing cell was compared with a pristine cell in cell performance. We also examined the performance change by pressing TiO₂ film, during cell fabrication, inside a high pressure chamber. Mostly, the change of conversion efficiency was compared for each cell, and an atomic force microscopy data were suggested to explain our results.

Key Words : DSSC, TiO₂, SWNT, CsSnI₃, Pressing technique

Introduction

Since 1991, dye-sensitized solar cells (DSSCs) have been improved due to their low fabrication cost and relatively high conversion efficiency.¹ Light-to-electron conversion efficiency of DSSCs was achieved over 10%,² which is still short of silicon's performance. DSSCs usually consist of a high porosity of nanocrystalline photoanode made of TiO₂ semiconductor deposited on a transparent conducting oxide (TCO) glass support and sensitized with a self-assembled monolayer of dye molecules anchored to the TiO₂ surface. When illuminated, the dye molecules capture the incident photons generating electron-hole pairs. The resultant electrons are immediately injected into the conduction band of the TiO₂ and transported to the electron-collecting counter electrode. Regeneration of dye molecules is accomplished by capturing electrons from a liquid electrolyte (iodide/iodine solution) or hole-transfer materials (CsSnI₃).

In the photovoltaic area, single-walled carbon nanotubes (SWNTs) are a promising material improving the performance of solar cells. Under ambient conditions, SWNTs are known as a p-type semiconducting material because adsorbed O₂ molecules on the surface of SWNTs withdraw electrons.³ Thus SWNTs can be used as a transporting material of holes, which could promote the separation of the generated electron-hole pairs.

Recently, the CsSnI₃ compound⁴ was developed as a hole-transporting material with n-type TiO₂ and the N719 dye (cis-diisothiocyanato-bis(2,2'-bipyridyl-4,4'-dicarboxylato)ruthenium(II) bis-(tetrabutylammonium)), and showed conversion efficiency up to 8.5% with a mask. Another group⁵ fabricated Schottky solar cells based on CsSnI₃ films which played a role as a light absorber. Solar cells made by the two

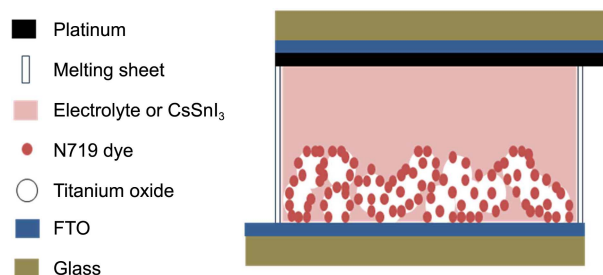


Figure 1. Schematic representation of dye-sensitized solar cell.

groups above were a new type of all-solid-state, inorganic solar cell system not using electrolytes.

In this study, SWNTs were incorporated with TiO₂ film, CsSnI₃ compound, and Pt film, separately, in Figure 1 in order to examine the role of SWNTs. Mostly, conversion efficiency was compared between samples, *i.e.*, cell containing SWNTs and cell not-containing SWNTs (pristine sample). We also pressed the sample by increasing gas pressure in a metal chamber, and compared efficiency and surface morphology by atomic force microscopy (AFM).

Experimental

TiO₂ Electrode and Counter Electrode. The TiO₂ paste consisted of TiO₂ powder (Degussa P25), polyethylene glycol, 10% acetyl acetone, DI-water, triton X-100 and was dispersed by sonicating for several hrs. TiO₂ films were prepared by spin coating of TiO₂ paste on ultra-cleaned fluorine-doped tin oxide (FTO, TEC-7 glass, Pilkington) substrate. The spin coating process was followed by sintering of the sample at 450 °C for 30 min in a furnace.⁶ The thickness of TiO₂ layer was controlled at 8.5 μm having the diameter of each particle to be 15-20 nm. The sintered TiO₂ film was immersed in ethanol solution containing 3 × 10⁻⁴ M N719 dye for 24 h at room temperature. The dye-adsorbed TiO₂

[†]This paper is to commemorate Professor Myung Soo Kim's honourable retirement.

film was washed with ethanol and dried under flowing nitrogen gas.⁴

The platinum counter electrode was prepared by spin coating of 5 mM solution of PtCl₄ in isopropanol on FTO glass and sintered at 400 °C for 15 min. Both counter and other electrodes were sealed with melting sheet (24 μm, Dupont). The average active area of each cell was about 0.4–0.5 cm².

CsSnI₃ and Electrolyte. Regeneration of dye molecules was accomplished by two methods, using a liquid electrolyte or hole-transfer materials (CsSnI₃). The electrolyte was prepared by sonicating DI-water/methanol (3:7) solution containing 0.5 M Na₂S, 0.125 M S powder, and 0.2 M KCl for 6 h.

Pure CsSnI₃ compounds were achieved by heating a stoichiometric mixture of CsI and SnI₂ in an evacuated pyrex at 450 °C for 30 min, followed by quenching to room temperature. CsSnI₃ powders were dissolved into anhydrous organic solvent like acetonitrile.⁴ The CsSnI₃ solution was injected into the cell by a micropipette and dried.

SWNT-containing Cells. Our cells containing SWNTs were fabricated mainly by three methods and their performances were compared with pristine cells; (sample 1) Mixing TiO₂ paste with SWNTs (SWNTs/TiO₂ powder = 0.001 wt %)⁷ (FTO/Pt/electrolyte/ N719 dye/TiO₂+SWNTs/FTO), (sample 2) Spraying SWNTs on the surface of Pt (SWNTs 0.01 mg on 0.4 cm² Pt) (FTO/Pt/SWNTs/N719 dye/electrolyte/TiO₂/FTO), (sample 3) Mixing CsSnI₃ with SWNTs (SWNTs/CsSnI₃ powder = 0.001 wt %) (FTO/Pt/CsSnI₃+SWNTs/N719 dye/TiO₂/FTO).

Results and Discussion

Figure 2(a) shows the cross section image of TiO₂ film on FTO glass. The length of the film was around 8.5 μm which gave the best efficiency to our cells. The film seemed to be flattened, but it was very porous in highly magnified surface image (Figure 2(b)).

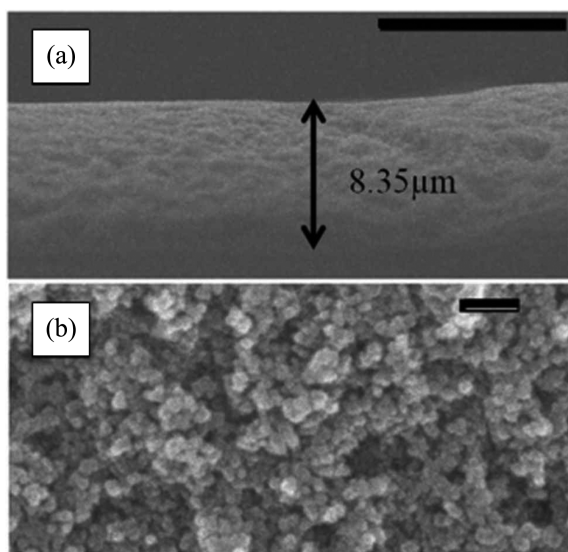


Figure 2. FE-SEM images of TiO₂ (a) cross (scale bar is 10 μm) and (b) surface section (scale bar is 100 nm).

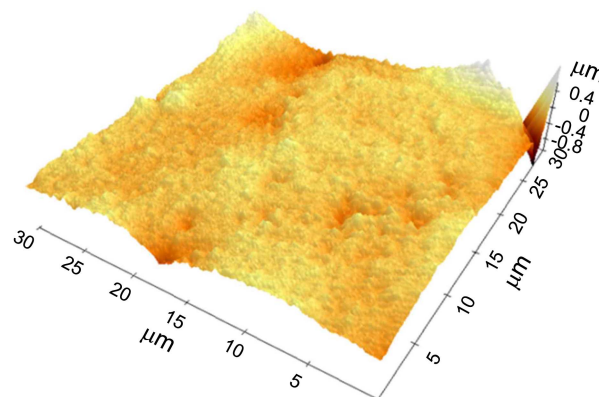


Figure 3. Atomic force microscopy (AFM) surface image of TiO₂ film.

Figure 3 shows 3-dimensional (3D) AFM picture and height distribution of the TiO₂ film. From the roughness distribution of surface of TiO₂, the root-mean square value (Rms) of the TiO₂ was determined to be 100.3 nm in a sample area of 30 × 30 μm². This value represented very high particle size for our TiO₂ compared to the previous TiO₂ film made by sol-gel and doctor-blade technique,⁸ where both showed Rms to be 0.35 and 23.94 nm, respectively.

Figure 4 shows the current density-voltage (J-V) curves for three samples, sample 1, 2 in section 2.3, and pristine cell. Again, sample 1 was made by mixing TiO₂ paste with SWNTs and sample 2 by spraying SWNTs on the surface of Pt. The amount of SWNTs was determined for each case to give the best conversion efficiency, respectively.

The results of Figure 4 are summarized in Table 1. The open-circuit voltages (V_{oc}) were in a similar range, 0.67–0.68

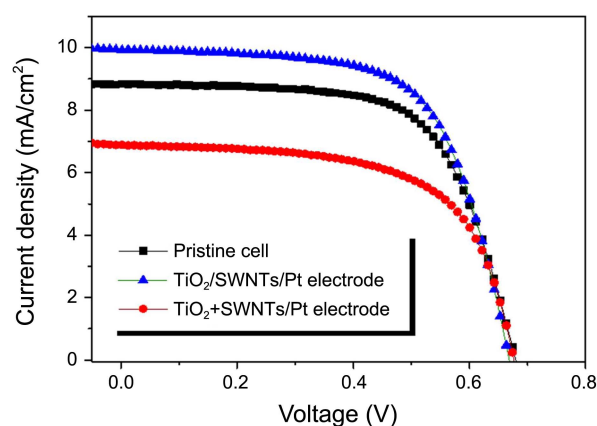


Figure 4. Current density-voltage curves of pristine cell (black squares), TiO₂ incorporated with SWNTs (red circles) and spraying SWNTs on the surface of Pt (blue triangles).

Table 1. Photovoltaic properties of pristine cell, TiO₂ incorporated with SWNTs (1) and spraying SWNTs on the surface of Pt (2)

Composition	V_{oc} (V)	J_{sc} (mA/cm ²)	FF (%)	E_{ff} (%)
Pristine cell	0.679	8.83	65.2	3.91
(1) TiO ₂ + SWNTs/Pt	0.676	6.88	61.7	2.86
(2) TiO ₂ /SWNTs/Pt	0.668	9.92	64.8	4.29

V for three samples. Sample 1 had the lowest value in short-circuit current (J_{sc}), fill factor (FF), and photo-current conversion efficiency (E_{ff}), and sample 2 showed the highest E_{ff} , 4.29%, which was increased at 9.7% compared with pristine cell. The main reason for this increase was attributed to the increasing J_{sc} .

According to the results of Nath *et al.*⁷ the homogeneous distribution of optimum amounts of carbon nanotubes (CNTs) into the mesoporous TiO_2 nanoparticles enhanced the conversion efficiency for cells with the optimized wt % of CNTs with respect to TiO_2 . Even though we changed the wt % of our SWNTs with respect to TiO_2 in a similar range of their conditions, results did not contribute positively. There were several differences between two groups, for example the thickness of TiO_2 (1 vs 8.5 μm), dispersing method of nanotubes into TiO_2 , and different kinds of nanotubes. We used purified SWNTs, but they did not mention the type and purification method of CNTs.

SWNTs are known as p-type semiconducting materials, *i.e.*, hole-transporting character under air condition, thus they can be supporting and/or suppressing materials for transporting each positive holes and negative electrons. The results of Figure 4 suggested that the SWNTs dispersing into TiO_2 and the SWNT film onto Pt electrode were located at the path of generated electrons and holes, respectively, resultantly they decreased and enhanced the E_{ff} by attributing control of currents in cells. In other words, p-type SWNTs could block the flow of generated electrons by locating at TiO_2 side, and reversely promote the flow of generated holes by locating at Pt side.

The absorbance and photoluminescence (PL) spectrum of the synthesized $CsSnI_3$ shown in Figure 5(a) had the same range and shape compared with those of the $CsSnI_3$ which was synthesized and characterized in ref. 9. Figure 5(a) also shows the comparison of absorbance of N719 dye+ TiO_2 and $CsSnI_3$ only on indium tin oxide (ITO). The absorbance of $CsSnI_3$ was comparable with dye+ TiO_2 , even higher at > 500 nm range. This indicated that our cells containing $CsSnI_3$ absorbed red and near-infrared light more efficiently than the cell without $CsSnI_3$.

Figure 5(b) shows the J-V performance of two cells, a cell using only $CsSnI_3$ and using $CsSnI_3$ mixed with SWNTs (sample 3 at section 2.3). J_{sc} was increased at 76% with the SWNTs, however E_{ff} was increased from 0.86 to 1.08 (25% increase). This result was mainly due to the linear shape of J-V curve in case of using SWNTs, *i.e.*, low FF and high series resistance. $CsSnI_3$ was developed to transport holes as a solid-state inorganic material to overcome the decomposition problem of a general electrolyte. Even though much higher currents were generated in our experiments by mixing SWNTs, the higher resistance should be reduced for future solar cells. We are investigating the reason.

The J-V curve was measured after pressing TiO_2 film of our pristine cell not including SWNTs. (FTO/Pt/electrolyte/N719 dye/ TiO_2 /FTO) The pressure was driven into the sonicated- TiO_2 film on FTO glass before sintering process. The pressing process was carried out inside home-made high

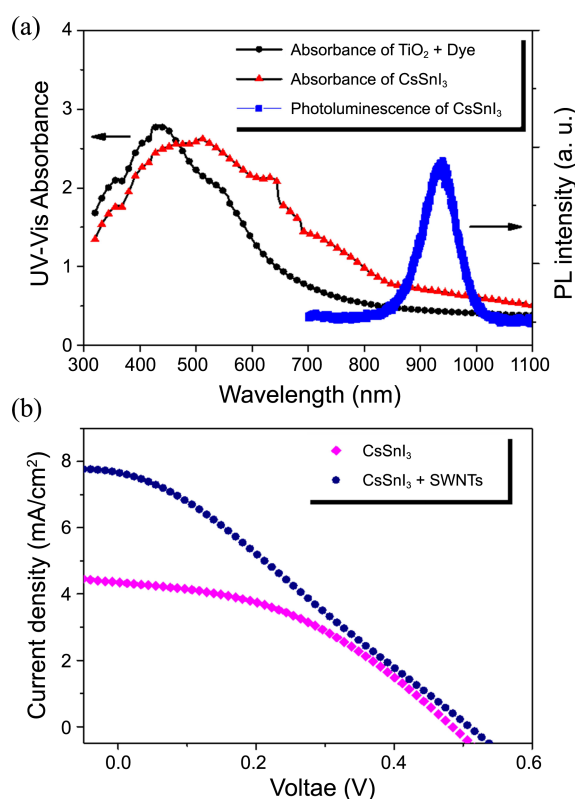


Figure 5. Optical absorbance of dye/ TiO_2 and $CsSnI_3$, photoluminescence of $CsSnI_3$ (a). Current density-voltage curves of the devices consisting of $CsSnI_3$ /dye/ TiO_2 (◆) and $CsSnI_3$ +SWNTs/dye/ TiO_2 (●) (b).

pressure chamber by using N_2 gas. Figure 6 shows the IV curve (a) of each sample and the plots ((b), (c), (d)) of each cell parameter. Interestingly, the whole parameters (E_{ff} , J_{sc} , and FF) were increased in our experimental range from atmosphere to 2, 4, 6 bar. V_{oc} (not plotted here) was around 0.7 V and was not changed for any sample. V_{oc} is generally

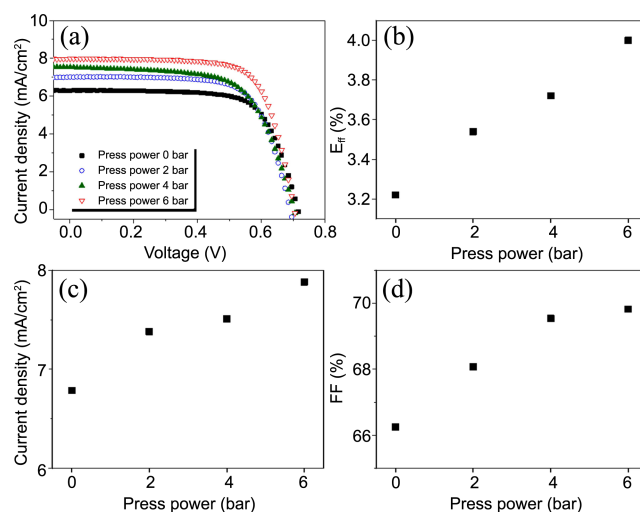


Figure 6. (a) J-V curves of each cell after pressing a sample. The change of photovoltaic properties with respect to increasing press power (0, 2, 4, 6 bar); (b) efficiency, (c) current density and (d) fill factor.

related to the energy level difference between an anode and a cathode. In our case, V_{oc} is proportional to the energy difference between the Fermi level of TiO_2 and Pt electrode. There were no reasons that V_{oc} was not changed after pressing the sample, since the same cathode and material were used for cell measurements. E_{ff} was increased highly among performance parameters at 24% ($E_{ff}=3.2 \rightarrow 4.0$).

The surface of TiO_2 was examined by AFM, giving a roughness (Rms) 100.3, 84.4, 73.3, and 56.5 nm for each cell. This result would not mean that the porosity was increased by driving higher pressure since the porosity was a function of number of holes as well as a roughness of a surface. Furthermore, the AFM results represented the characteristic feature of the TiO_2 surface only, not inside a bulk of TiO_2 . From the AFM results, it would be suggested that highly well-ordered TiO_2 film was formed by increasing pressure. More analytical tools are under investigation to know the distribution and the depth profile of nanoparticles inside TiO_2 using tunneling electron microscopy and Auger spectrophotometer.

Conclusion

DSSC was fabricated with nanocrystalline TiO_2 film electrode on FTO glass, N719 dye, electrolytes, and counter Pt electrode. Conversion efficiency decreased when TiO_2 mixing with SWNTs, on the while, increased when depositing SWNT film on Pt electrode compared with pristine cell. It was interpreted that SWNTs were acting as a barrier layer for negative electrons and as a supporting layer for positive

holes, respectively, due to their p-type character. We also found that J_{sc} was increased greatly with the SWNTs combining with hole-transporting material, $CsSnI_3$, instead of electrolytes. By pressing the TiO_2 film during cell fabrication, cell efficiency was also increased from 3.2 to 4.0%.

Acknowledgments. This paper is dedicated to Professor Myung Soo Kim on the occasion of his honourable retirement. This paper was supported by the National Research Foundation of Korea Funded by the Ministry of Education, Science, and Technology (KRF-2011-0028850).

References

1. O'Reagan, B.; Grätzel, M. *Nature* **1991**, 353, 737.
2. Yella, A.; Lee, H. W.; Tsao, H. N.; Yi, C.; Chandiran, A. K.; Nazeeruddin, M. K.; Diau, E. W. G.; Yeh, C. Y.; Zakeeruddin, S. M.; Grätzel, M. *Science* **2011**, 4, 629-634.
3. Bockrath, M.; Hone, J.; Zettl, A.; McEuen, P. L.; Rinzler, A. G.; Smalley, R. E. *Phys. Rev. B* **2000**, 61, R10606.
4. Chung, I.; Lee, B. H.; He, J.; Chang, R. P. H.; Kanatzidis, M. G. *Nature* **2012**, 485, 486.
5. Chen, Z.; Wang, J. J.; Ren, Y.; Yu, C.; Shum, K. *Appl. Phys. Lett.* **2012**, 101, 093901.
6. Lee, Y. L.; Lo, Y. S. *Adv. Funct. Mater.* **2009**, 19, 604.
7. Nath, N. C. D.; Sarker, S.; Ahammad, A. J. S.; Lee, J. J. *Phys. Chem. Chem. Phys.* **2012**, 14, 4333.
8. Arabatzis, I. M.; Antonaraki, S.; Stergiopoulos, T.; Hiskia, A.; Papaconstantinou, E.; Bernard, M. C.; Falaras, P. *J. Photochem. Photobiol. A* **2002**, 149, 237-245.
9. Shum, K.; Chen, Z.; Qureshi, J.; Yu, C.; Wang, J. J.; Pfenninger, W.; Vockic, N.; Midgley, J.; Kenney, J. T. *Appl. Phys. Lett.* **2010**, 96, 221.